

Responses to the Comments made by Referee #2

Ranil Basnayake, Erik Bollt, Nicholas Tufillaro, Jie Sun, and Michelle Gierach

April 29, 2017

We thank the reviewer for valuable comments. We highlighted the changes in the revised version of the manuscript using a [blue font](#).

Referee #2: *The paper is overall well-written and describes how to deal with an important problem when using remote sensing data, especially for using infrared and visible frequencies for satellite imagery, that of striping. The paper presents a method which is able to diminish and correct the impact of striping.*

Response: Thank you for providing positive comments about our work.

Referee #2: *Despite some minor grammar and orthographic errors, the paper is well-written, explains the problem clearly, presents the method in a clean manner and provides a sufficient amount of details of it.*

Response: We agree, our original version had grammar and orthographic errors. Hopefully the current version is free of those errors. We have highlighted the corrections in [blue](#) in the revised version.

Referee #2: *My only real concern with this paper is its suitability for Nonlinear processes in geophysics, as no nonlinear geophysical process is described in all the paper, just a processing technique (interesting as it is).*

Response: We considered NPG as a suitable outlet for our paper especially because of the journal's statement that "The editors encourage submissions that apply nonlinear analysis methods to both models and data." In this regard, we feel that our paper makes a good candidate for this journal. In addition, this paper concerns a data issue regarding remote sensing in the field of geoscience. Both referees have responded positively to this paper, and we believe the general readership will as well. Therefore it is our opinion that experimental issues related to the theme of the journal are a good topic for publication here, and we hope the editor and referees will agree with this point.

Some minor comments:

Referee #2: *How is the direction of stripes identified in general?*

Response: The stripes are due to details of the optical sensor on board the satellite camera. Therefore the exact alignment of this cause of the stripes is well known by the known orientation of the satellite.

Referee #2: *What happens if the stripes contain valid information, i.e., there is an offset and/or a rescaling? Shouldnt they be consider, after readjustement?*

Response: This a good question. If an actual stripe contains valid information, we are not able to do any readjustement in our destriping model. On the other hand, if the real data appears as a stripe, then the question can be broken into two parts.

1. If there is a road, or any real signal that is exactly aligned with axis of the known stripes biased in a part of the image (assume that we have a part of the image with only biased data). In this case, we can destripe the image by defining the weight matrix L , considering a piece of image that does not have the horizontal road. We have added an explanation in page 3 for that.
2. If there is a road, or any real signal that is exactly aligned with axis of the known stripes biased in the complete image. Then they would be in danger of being regularized to disappear in a smooth denoised image and our only current protection against this is the unlikeliness that a perfectly straight road would be both straight for long stretches, and furthermore straight and aligned with the sensor error. If this were deemed a general problem however, a mask to de-emphasize the regularization spatially could be developed in the regularity term at spatial locations where there is a known mapped road or other perfectly straight feature.

Referee #2: 1) *Eq. 9 has more undetermination than just a constant value: any function in the kernel of the operator $D_{xx} + \alpha L D_{yy}$ can be added to a solution and will yield a new solution. In fact, the point is that the matrix A is non-invertible. This is connected with the discussion on condition numbers in Section 2.3, but prior to go directly to discuss any regularization I think this point deserves some comments.*

Response: This is an excellent comment. We'd like to clarify that even though the matrix A appears non-invertible, with a non-empty kernel, in this work we have imposed "reflexive" boundary conditions parallel to the stripes and "zero" boundary conditions transverse to the stripes which makes A a full-rank matrix, thus leading to uniqueness of solution. This important issue is now explicitly discussed on page 4, (1) last sentence of the first paragraph, (2) in the paragraph immediate above Section 2.1.

Referee #2: 2) *The issue is significant for instance on page 7, when developing the U-curve method, as one important parameter is the minimum non-zero singular value. How do you decide that some value is non-zero for a given numerical precision? A threshold is for sure used, and the point should be clarified, explaining in particular this choice.*

Response: Thank you for raising this question and it helped us to provide correct notations for the definition of U -curve method. We have changed the notations in Eq. (11), Eq. (12) and 5th line in page 6. In this computation, we used 10^{-12} as the smallest value in the selection interval of α . In this way, we can give the threshold for the smallest singular value to be larger than 10^{-18} as we can find an appropriate $\alpha \in (\sigma_r^{2/3}, \sigma_1^{2/3})$.

Referee #2: 3) *Chlorophyll images are not as smooth as claimed, chlorophyll concentration being very intermitten. Even SST present strong frontal zones that break smoothness. Along fronts they are indeed smooth, but not across fronts, so anisotropy is a key ingredient. Some problems may arise with the parte of the front that is eventually aligned with the stripe direction. Please comment the issue.*

Response: We agree that the images are not always smooth and hence the computation of S curve may be affected by non-smoothness of the images. In this case, we should not pick the whole image to compute the S curve, but an image segment that is smooth enough to identify the stripes from the S curve. We have explained it in second paragraph of Section 3.2 (page 11-12).

Referee #2: 4) *The absolute percentage error on page 10 is not correctly defined, as referring to a value with a conventional origin is meaningless (imagine how this error would change if you take the SST in Kelvin or in Celsius, for instance). It is much more customary to compare errors to the dynamic range of the image (for instance, as measured by the standard deviation of the values).*

Response: We agree that the “absolute percentage error” is not invariant. However, in this work, we try to define an error metric that can be used to visualize the error between the striped and destriped images. When we work with real world data, we can only compare the data which are not on the stripes and this “absolute percentage error” shows us how the computations affect such data. Therefore, we believe that this definition works well for our purpose.

Referee #2: *12 is not a magic number; please be more descriptive about how to choose the threshold in figure 5. And please provide units.*

Response: Thank for pointing out this and the correct number should be 18. We have included an explanation for that in page 10. Also thank you for reminding us to put the units for the threshold value and it will definitely help the reader to understand the concept of the S curve. We have added units with explanations at the 5th line in page 10, Fig. 5, 2nd line in page 12 and 5th line in page 15.

Referee #2: *Although it is a bit beyond of the scope of the paper, it will be very convenient to have an in-situ validation dataset for verifying if the destriped images are of higher quality.*

Response: Thank you for suggesting a data set for the validation and absolutely it is beyond of the scope of the paper. We will surely try it in our future work.

Regularization Destriping of Remote Sensing Imagery

Ranil Basnayake^{1,2}, Erik Bollt^{1,2}, Nicholas Tufillaro³, Jie Sun^{1,2}, and Michelle Gierach⁴

¹Department of Mathematics, Clarkson University, Potsdam, NY 13699, USA

²Clarkson Center for Complex Systems Science (C^3S^2), Potsdam, NY 13699, USA

³College of Earth, Ocean, and Atmospheric Sciences, Oregon State University, Corvallis, OR 97331, USA

⁴Jet Propulsion Laboratory, California Institute of Technology, Pasadena, CA, 91109, USA

Correspondence to: Ranil Basnayake (rbasnaya@clarkson.edu)

Abstract. We illustrate the utility of variational destriping for ocean color images from both multispectral and hyperspectral sensors. In particular, we examine data from a filter spectrometer, the Visible Infrared Imaging Radiometer Suite (VIIRS) on the Suomi National Polar Partnership (NPP) orbiter, and an airborne grating spectrometer, the Jet Population Laboratory's (JPL) hyperspectral Portable Remote Imaging Spectrometer (PRISM) sensor. We solve the destriping problem using a variational regularization method by giving weights spatially to preserve the other features of the image during the destriping process. The target functional penalizes 'the neighborhood of stripes' (strictly, directionally uniform features) while promoting data fidelity, and the functional is minimized by solving the Euler-Lagrange equations with an explicit finite difference scheme. We show the accuracy of our method from a benchmark data set which represents the Sea Surface Temperature off the Coast of Oregon, USA. Technical details, such as how to impose continuity across data gaps using inpainting, are also described.

10 1 Introduction

Striping is a persistent artifact in remote sensing images and is particularly pronounced in Visible-Near Infrared (VNIR) water-leaving radiance products such as those produced by operational sensors including NPP VIIRS, Landsat 8 Operational Land Imager (OLI), and Geostationary Ocean Color Imager (GOCI), as well airborne instruments such as NASA's JPL PRISM sensor. These sensors cover a temporal sampling range from daily (VIIRS) to hourly (GOCI), and spectral sampling from multi-spectral (VIIRS, GOCI) to hyperspectral (PRISM). Striping is pronounced in products from all these sensors because atmospheric correction for ocean color products typically removes at least 90% of the signal recorded at the Top of Atmosphere (TOA). Put another way, any artifacts in the TOA signal are amplified by at least a factor of 10 in any derived water products such as normalized water leaving radiance of a specific spectral band ($nLw(\lambda)$), or in product fields such as total suspended sediment (TSS) concentration maps.

20 Striping is ubiquitous and difficult to remove because it has many possible origins. The detectors themselves are subjected to small amplitude variations in both sensitivity and calibration. The view angles (azimuthal and zenith) also vary from detector to detector and from pixel to pixel. Other differences in the instrument's optical path, components (e.g. mirrors), asynchronous readout, and so on, also cause striping. Not unexpectedly, the magnitude of the striping varies from image to image. Striping is

particularly problematic when comparing a sequence of images, since any difference in computations between images produces spurious results in the neighborhood of stripes.

Ocean products from NPP VIIRS have shown problematic striping since its launch, which has led to ~~focused~~ focus efforts at both NASA and NOAA to find ~~corrections~~ correction methods. NASA created a vicarious destriping method for VIIRS
 5 images based on a collection of long term on-orbit image data, including solar and lunar calibrations. NASA's Ocean Biology Processing Group (OBPG) began serving operational products with their vicarious calibrations and destriping for VIIRS in 2014 ?. In contrast, a method for hierarchically destriping VNIR images based on a single scene ~~,-using-a-hierarchical-approach,~~ was proposed in ?. This particular variational method was more recently augmented with filtering using a hierarchical image decomposition ?, and that algorithm has also been implemented by scientists at NOAA for operations with images from
 10 VIIRS ?? . Scene based processing methods are advantageous for sensors which do not have dedicated calibration subsystems such as a solar diffuser, or where the data sets are limited in scope (such as airborne sensors) and do not include uniform scenes for vicarious calibration.

2 Regularization Destriping: the Functional and its Minimization

The method described here is closely related to the destriping functional described in ?. Our work differs in its exact func-
 15 tional form, and its ~~method~~ principle of solution. In particular, we formulate a solution for destriping in an inverse-problem framework, and keep only the part of the functional in ? that smooths the stripes. This new formulation allows us to provide an explicit numerical solution instead of an iterative one, the former being more efficient thus better suited for operational codes. We explicitly introduce a regularization parameter that controls the relative balance between the data term ("fitting the original image") and the regularity term ("smoothing out the stripes"). ~~Solutions of this kind are~~ Such regularization is a common prac-
 20 tice in inverse problems ?, and fall under the rubric of Tikhonov regularization theory. As a further improvement to refinement of the destriping functional, we specifically define weights for the regularization term so that the algorithm applies only to the stripes while preserving the other features.

Assuming that the stripes are parallel to one another in the image plane, we take the direction of the stripes as the x (horizontal) direction. Thus the data term representing the horizontal gradient difference between the original and the destriped
 25 images is given as

$$E_D(u) = \int_{\Omega} \left(\frac{\partial}{\partial x} (u - f) \right)^2 d\Omega, \quad (1)$$

where Ω is the image domain on xy plane, $f(x, y)$ is the original image with stripes, and $u(x, y)$ is the destriped image.

The regularization term emphasizes the smoothness in the vertical direction, which is assumed to be free of stripes. This regularization term is given by

$$30 \quad E_R(u) = \int_{\Omega} \left(\frac{\partial u}{\partial y} \right)^2 d\Omega. \quad (2)$$

The regularization parameter $\alpha > 0$ balances the data term and the regularization term. The resulting destriping functional is

$$E_C(u) = \int_{\Omega} \left(\frac{\partial}{\partial x}(u - f) \right)^2 d\Omega + \alpha \int_{\Omega} \left(\frac{\partial u}{\partial y} \right)^2 d\Omega. \quad (3)$$

This is the x -directional destriping functional proposed by Bouali in ?, and it is equivalent to the basic form of our destriping functional when $\alpha = 1$. The choice of α , as we show later, is key to achieving the balance ~~of~~ between matching the original image and removing stripes. However, our approach differs from ? and our goal is to develop a destriping method ~~which~~ that is easy to implement while preserving the other features of the image.

A drawback of scene-based destriping are unintended changes in the values of all the pixels and not just the stripes. If we apply the regularization term for the whole image as it is in Eq. (3), the entire image is effected. This could modify the original features of the image, in addition to recovering stripes. Therefore, we further develop our functional in Eq. (3) to regularize only the stripes. We introduce a mask (L) to the regularization term, to limit the smoothing ~~affects~~ effects to the stripes. To obtain L from the image, we first compute the slope of the image transverse to the stripes using first order finite differences. Then we sum the absolute differences parallel to the stripes. This yields the total value (S) corresponding to each row. From the peaks of graph S ~~vs~~ versus r , where r is the row index, we can identify the stripes and select a ~~threshold~~ “threshold” to separate the stripes from the other features. To compute the S curve, we do not need to consider the complete image and instead we can consider a vertical image segment that contains some part of all the biased data. In this case, we can preserve the actual features such as roads or any other real signals that are exactly aligned with stripes.

The mathematical expression for the computation of S for an image f , of size m -by- n , with ~~suitable~~ a suitable boundary condition, can be written as

$$S(r) = \sum_{c=1}^n |f(r, c) - f(r + 1, c)|, \quad (4)$$

where $r = 1, 2, \dots, m$ and $f(m + 1, c)$ is the introduced boundary row. Now defining the ~~threshold value from~~ “threshold” value from the S curve, we obtain the sparse matrix L ~~with ones~~ indicating by assigning “ones” for the locations of the stripes. We will explain the procedure of selecting an appropriate “threshold” value using examples in Sec. ??. Any row r , where $r = 1, 2, \dots, m$ of matrix L with size m -by- n can be defined as

$$L(r, c) = \begin{cases} 1, & \text{if } S(r) \geq \text{threshold} \\ 0, & \text{otherwise,} \end{cases} \quad (5)$$

where $c = 1, 2, \dots, n$.

Then the new destriping functional, with the spatially weighted regularization term, is written as

$$E(u) = \int_{\Omega} \left(\frac{\partial}{\partial x}(u - f) \right)^2 d\Omega + \alpha \int_{\Omega} L \left(\frac{\partial u}{\partial y} \right)^2 d\Omega. \quad (6)$$

The destriped image is obtained by minimizing the functional after choosing an appropriate regularization parameter. Note that the functional $E(u)$ is invariant under constant shift. That is, $E(u+a) = E(u)$ for any constant a , implying that minimization of $E(u)$ leads to an infinite number of solutions. ~~Because we want to keep the average intensity of the original and the destriped images the same, we assert $\langle u \rangle = \langle f \rangle$~~ In this work, we impose appropriate boundary conditions (as discussed below)

5 that ensure uniqueness of the solution.

We create a destriped image by minimizing the energy functional in Eq. (6) using the Euler-Lagrange equation. For a functional of the form

$$J(u) = \int_{\Omega} F(x, y, u, u_x, u_y) d\Omega,$$

on the bounded domain Ω , the Euler-Lagrange equation is given as

$$10 \frac{\partial F}{\partial u} - \frac{\partial}{\partial x} \left(\frac{\partial F}{\partial u_x} \right) - \frac{\partial}{\partial y} \left(\frac{\partial F}{\partial u_y} \right) = 0. \quad (7)$$

~~Applying~~ As explained in ??, the Euler-Lagrange equation,

$$\underline{u_{xx} + \alpha L u_{yy} = f_{xx}} \quad (8)$$

is obtained by applying Eq. (7) to Eq. (6), ~~the Euler-Lagrange equation, as explained in ?? is the partial differential equation~~

$$\underline{u_{xx} + \alpha L u_{yy} = f_{xx}},$$

15 where subscripts represent the argument variable(s) of the partial derivatives. We can rewrite ~~the~~ Eq. (8) as

$$(D_{xx} + \alpha L D_{yy}) u = D_{xx} f, \quad (9)$$

where ~~the~~ operators $D_{\bullet\bullet}$ are two dimensional arrays of size $k \times k$ used to compute the partial derivatives of a given vector of size $k \times 1$ with respect to the indices $\bullet\bullet$.

We use finite difference approximations with suitable boundary conditions for each derivative to directly represent these

20 differential operators. In this work, we apply “reflexive” boundary conditions parallel to the stripes and “zero” boundary conditions transverse to the stripes when we the generate derivative operators. These boundary conditions lead $(D_{xx} + \alpha L D_{yy})$ to a full rank operator and hence we reach a unique solution. In Eq. (9) we stack the given image of size $p \times q$ ~~onto~~ into $k \times 1$

vector, where $k = pq$. We can now use the differential operators to write the linear Euler-Lagrange equation in the form of $Au = b$, and solve for u using an appropriate numerical method rather than solving the Euler-Lagrange equation for u from an

25 iterative scheme such as Gradient decent method.

2.1 Construction of the Differential Operator

We construct the operator D_{xx} using finite difference approximations. The operator D_{yy} is built by taking the transpose of the finite difference stencil. Suppose we have a function $M(x, y) \in \mathbb{R}^{p \times q}$. We need to compute the second order partial derivative

of M with respect to x . We use a fourth-order finite difference approximation and compute the point-wise second partial derivative of the array M with respect to x .

As an example, take an array $M(x, y)$ of size 3×5 where we want to compute $M_{xx}(x, y)$. We index the elements in the array in the form of a column vector as shown in Table 1, with two added boundary columns for each side.

Table 1. An array of 3×5 with boundary points in **redbold**

m₄	m₁	m_1	m_4	m_7	m_{10}	m_{13}	m₁₃	m₁₀
m₅	m₂	m_2	m_5	m_8	m_{11}	m_{14}	m₁₄	m₁₁
m₆	m₃	m_3	m_6	m_9	m_{12}	m_{15}	m₁₅	m₁₂

115 The boundary points are highlighted in **redbold**. If we compute the partial derivative of m_1 with respect to x , the resulting approximation is **obtained as-**

$$\frac{\partial^2 m_1}{\partial x^2} = \frac{1}{12h^2} [-\mathbf{m}_4 + 16\mathbf{m}_1 - 30m_1 + 16m_4 - m_7] = \frac{1}{12h^2} [-14m_1 + 15m_4 - m_7].$$

~~Continuing this manner for all the elements~~ Computing the finite difference approximations for each element in the array, we
 120 can compute-obtain the differential operator D_{xx} . ~~Using a multiplication factor of $12h^2$, we obtain a corresponding to the 3×5 array in Table ??.~~ The resulting operator is a sparse matrix with only five non-zero diagonals (Table ??) and it is shown in Table ?? with a multiplication factor of $12h^2$.

~~Similarly, D_{yy} and the other derivatives can be estimated as needed. The boundary points are highlighted as bold entries. If we compute the partial derivative of m_1 with respect to x , the resulting approximation is obtained as-~~

$$125 \frac{\partial^2 m_1}{\partial x^2} \equiv \frac{1}{12h^2} [-\mathbf{m}_4 + 16\mathbf{m}_1 - 30m_1 + 16m_4 - m_7] = \frac{1}{12h^2} [-14m_1 + 15m_4 - m_7].$$

~~Continuing this manner for all the elements, we can compute the differential operator D_{xx} . Using a multiplication factor of $12h^2$, we obtain a sparse matrix with only five non-zero diagonals (Table ??).~~

2.2 Solution to the Euler-Lagrange Equation

130 Now we can determine the solution to Eq. (9). We rewrite the Eq. (9) as

$$Au = b, \tag{10}$$

where $A = D_{xx} + \alpha LD_{yy}$ and $b = D_{xx}f$. If the size of the given striped image f is $p \times q$, then A is a $k \times k$ sparse array and b is a $k \times 1$ array, where $k = pq$.

Table 2. A discretized derivative operator $D_{xx} \times 12h^2$ for a 3×5 matrix.

	m_1	m_2	m_3	m_4	m_5	m_6	m_7	m_8	m_9	m_{10}	m_{11}	m_{12}	m_{13}	m_{14}	m_{15}
m_1	-14	0	0	15	0	0	-1	0	0	0	0	0	0	0	0
m_2	0	-14	0	0	15	0	0	-1	0	0	0	0	0	0	0
m_3	0	0	-14	0	0	15	0	0	-1	0	0	0	0	0	0
m_4	15	0	0	-30	0	0	16	0	0	-1	0	0	0	0	0
m_5	0	15	0	0	-30	0	0	16	0	0	-1	0	0	0	0
m_6	0	0	15	0	0	-30	0	0	16	0	0	-1	0	0	0
m_7	-1	0	0	16	0	0	-30	0	0	16	0	0	-1	0	0
m_8	0	-1	0	0	16	0	0	-30	0	0	16	0	0	-1	0
m_9	0	0	-1	0	0	16	0	0	-30	0	0	16	0	0	-1
m_{10}	0	0	0	-1	0	0	16	0	0	-30	0	0	15	0	0
m_{11}	0	0	0	0	-1	0	0	16	0	0	-30	0	0	15	0
m_{12}	0	0	0	0	0	-1	0	0	16	0	0	-30	0	0	15
m_{13}	0	0	0	0	0	0	-1	0	0	15	0	0	-14	0	0
m_{14}	0	0	0	0	0	0	0	-1	0	0	15	0	0	-14	0
m_{15}	0	0	0	0	0	0	0	0	-1	0	0	15	0	0	-14

Using a suitable value for the regularization parameter, Eq. (??) can be solved as a linear system. The system is sparse and hence the computation time for an image with n pixels is of $O(n)$ for each iteration. Clearly, at this stage, for a given α , Eq. (??) is straightforward to solve, however in terms of the image processing, the specific choice of α plays an important role. To achieve “the most appropriate solution,” we need to determine the best regularization parameter α .

2.3 Selection of the Regularization Parameter

The condition number of the resulting matrix quantifies the amplification of computational errors seen while solving the problem by direct computation. The condition number may be computed as the ratio between the largest singular value and the smallest singular value of the coefficient matrix. If the condition number is large, then the coefficient matrix is said to be ill-conditioned and hence the corresponding system is ill-posed. In an ill-posed system, the solution is highly sensitive to perturbations of the input data. Regularizing an ill-posed system, emphasizing a desired property of the problem, introduces a stable way to define a desirable solution ????. This is the standard trade-off between regularity and stability in Tikhonov regularization terms.

We regularize our computed solution by emphasizing the expected physics. To damp the accumulated errors from the residuals, we must make sure that we add sufficient regularity. The balance between the data term and the regularization term is very important: if we add too much regularity, it will divert the solution from the desired solution. Stated in terms of Tikhonov regularization, α serves the role to select a unique optimizer u , from what would be and otherwise ill-posed system had only the data fidelity had been chosen. In terms of the images, the data fidelity states that the optimizer image u should “appear as”

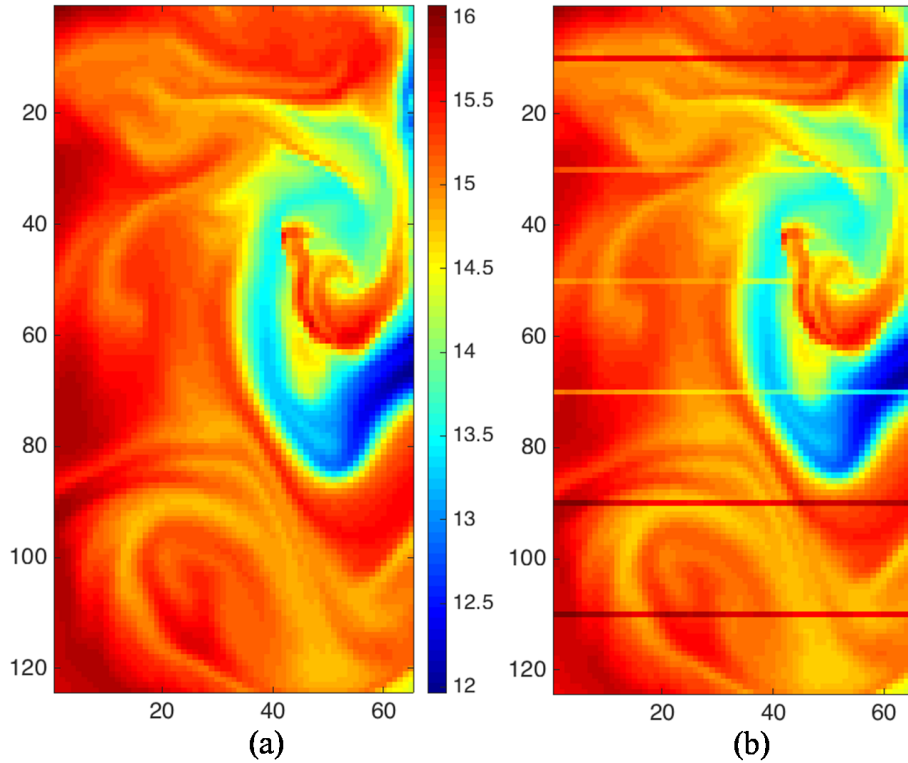


Figure 1. Image (a) shows (simulated) variations of Sea Surface Temperature off the coast of Oregon, USA on 1 August 2002. The image was generated from a Regional Ocean Model System (ROMS, Courtesy of John Osborne, Oregon State University), using the data [assimilation](#) from the Geostationary Operational Environmental Satellite (GOES). Image (b) is created by adding artificial stripes every 20th row.

The S curve corresponding to the SST image is shown in graph (a) in Fig. ?? . The “threshold” value for this problem is also shown on [the](#) same graph and it is ~~12-18~~ in this case. [If we consider the units of the Sea Surface Temperature data, the threshold value can written as \$842 C^{\circ} longitude/latitude\$. To determine the best “threshold” value that does not affect to the image regions with no stripes, we begin the procedure by assigning the “threshold” value to the maximum peak of the \$S\$ curve. Then we apply the destriping algorithm and check the solution. If at least one stripe is still visible, we assign the next highest peak of the \$S\$ curve as the “threshold” value and check for the stripes. Continuing this manner until all the stripes are removed, the best “threshold” value can be determined.](#) The peak points that ~~has-crossed-by~~ [have crossed](#) the threshold value are the stripes. As a comparison of the full destriping image, the absolute percentage error between the striped and ~~destriped~~ [destriped](#) image is shown in the image (b) in Fig. ?? . This is computed by,

$$\text{Absolute Percentage Error} = \frac{|f - u|}{f} \times 100,$$

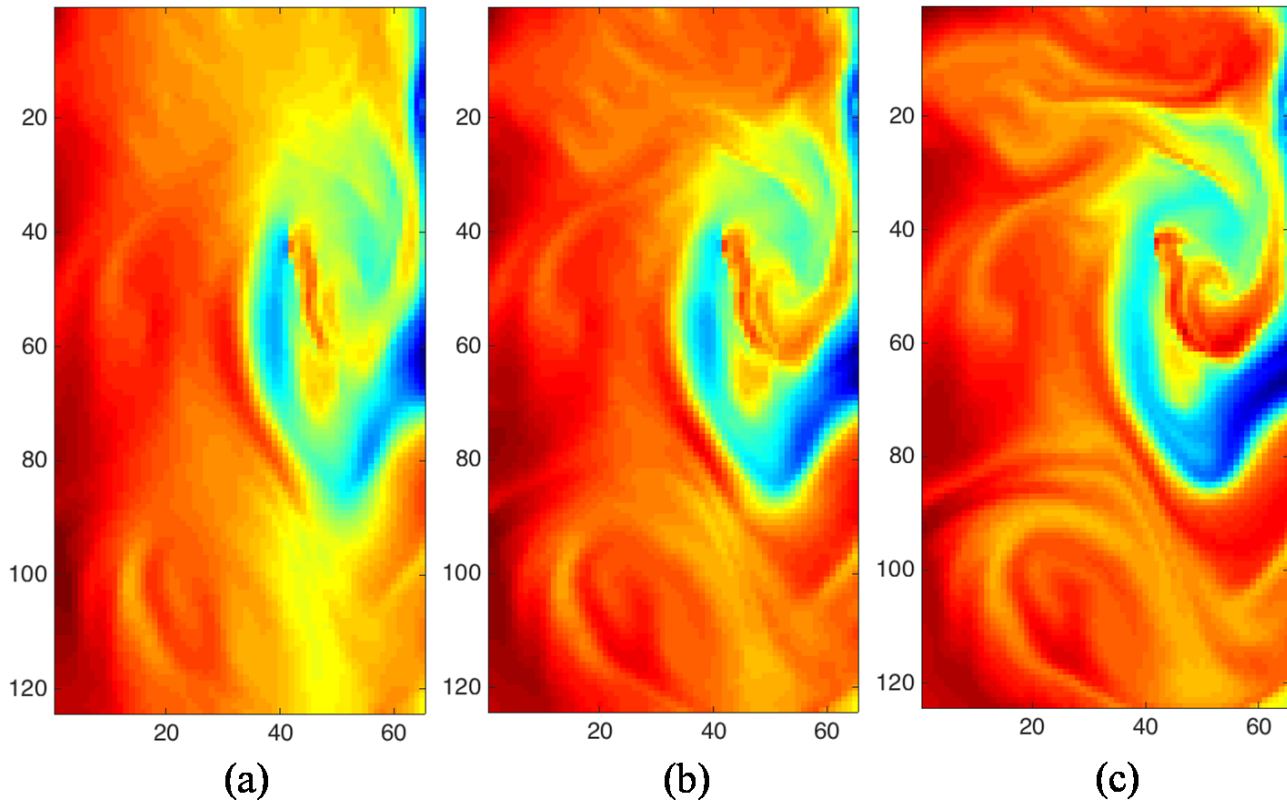


Figure 2. These three images represent the destriped image of the image shown in Fig. ??(b) from three different ways. Image (a) and (b) are obtained with $\alpha = 1$ and $\alpha = 3 \times e^{-1} \approx 3 \times 10^{-1}$ from the functional in Eq. (3). Image (c) is obtained with $\alpha = 7 \times e^{-1} \approx 7 \times 10^{-1}$ from the functional with spatially weighted regularization term as shown in Eq. (6).

205 1-2093.

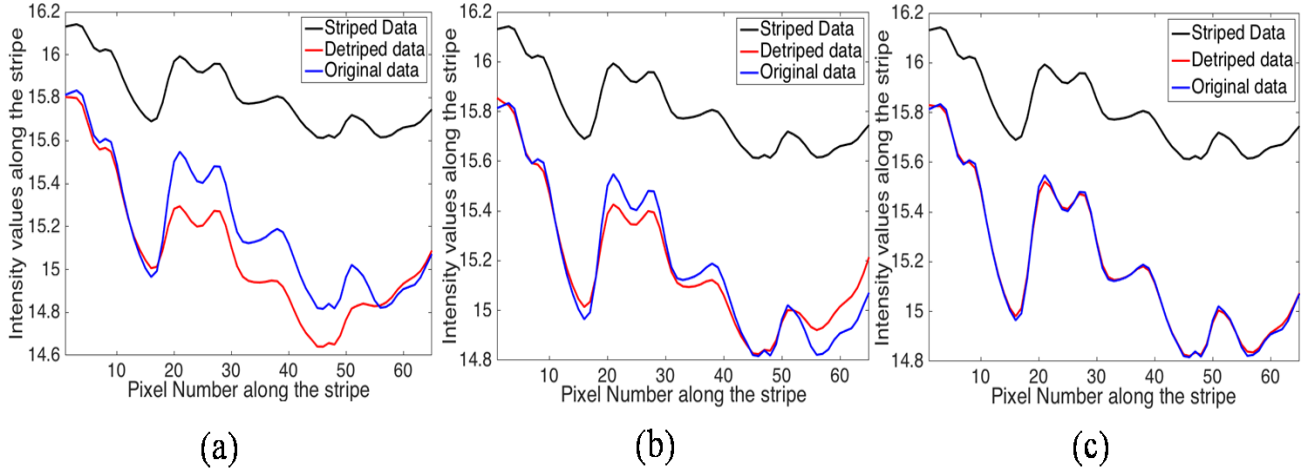


Figure 3. This figure presents three different reconstructions of the stripe at the 110th row of the image shown in Fig. ??(b). The graphs show the actual data in blue, striped data in black and the detriped data in red. Graphs (a) and (b) represent the reconstructions from the functional in Eq. (3) with $\alpha = 1$ and $\alpha = 3 \times 10^{-1}$, respectively. The graph (c) shows the reconstruction from the functional in Eq. (6) with $\alpha = 7 \times 10^{-1}$.

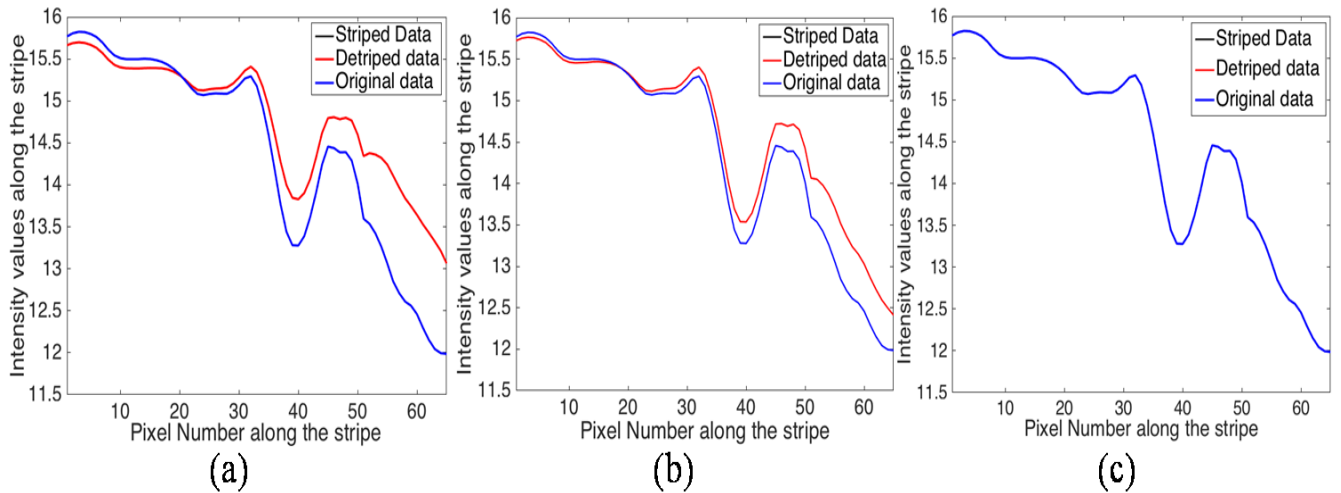


Figure 4. This figure shows the effects of destriping on the places where ‘no stripes’. We randomly picked the 67th row for this comparison. When $\alpha = 1$ in the un-weighted regularization functional, the image is more smoothed and affects destriping to the whole image. Much better results can be obtained from the the un-weighted regularization functional with $\alpha = 3 \times 10^{-1}$ which is the U -curve solution and shown in graph (b). Spatially weighted regularization term with $\alpha = 7 \times 10^{-1}$ provides less effect to the other features of the image and we can observe that from the graph (c).

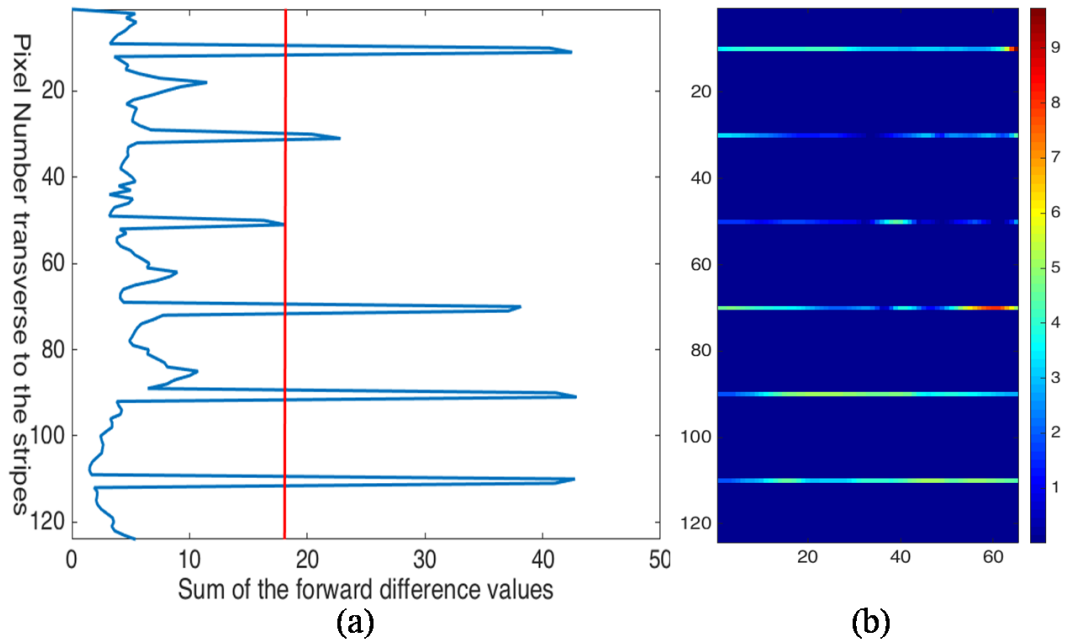


Figure 5. Image (a) shows the S function values against the column numbers. The peak points represent the stripes. When “`threshold`” is set at `18`, only stripes can be included for the regularization but excludes all the other features of the image. With the units of the image data, the threshold value can written as $842 C^\circ \text{longitude/latitude}$. Then the percentage error between the striped and destriped image are shown in the image (b). The error where there are no stripes is always closer to the zero

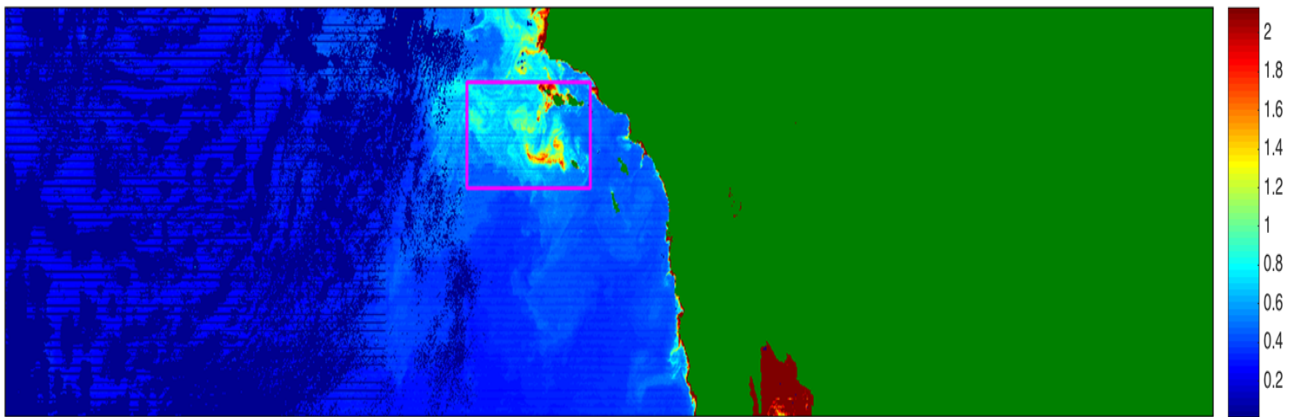


Figure 6. The image shows the chlorophyll concentration in $mg/(m^3)$ near the Santa Monica region in Southern California as viewed by VIIRS on November 07, 2014. Green represents the land and dark blue represents the dropped data due to bow-tie effects and missing data due to clouds. For a detailed discussion, we next consider the subset of the image that is covered by the pink square in the image.

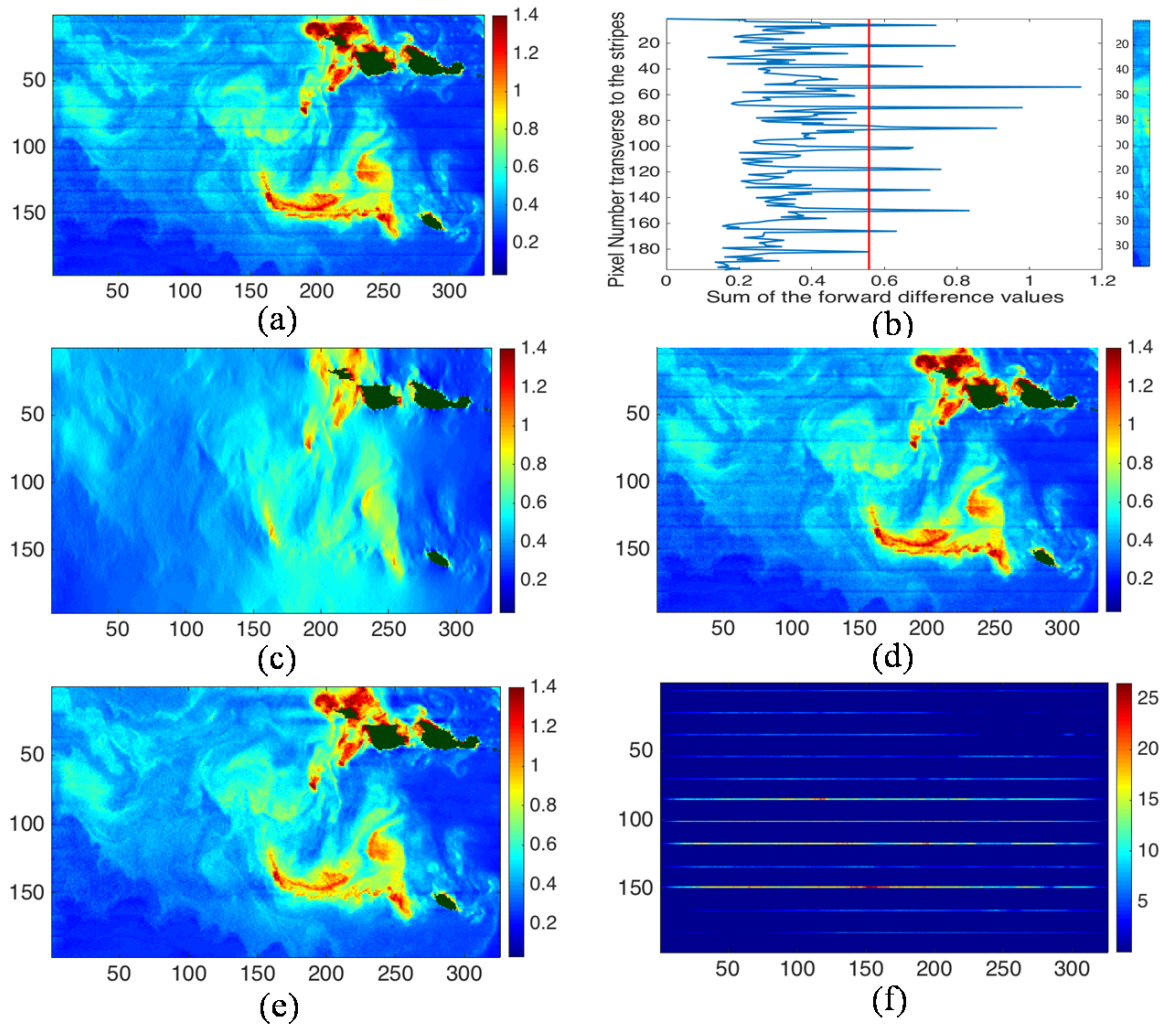


Figure 7. Image (a) shows the cropped region shown in Fig. ?? and the graph (b) shows the S curve with the threshold and the image piece (columns 137 to 148) that we used compute the values of S curve. The images (c), (d) and (e) represent the destriped images of (a) with $\alpha = 1$ with unweighted regularization term and $\alpha = 10^{-5}$ and $\alpha = 10^{-2}$ with weighted regularization term respectively. Image (e) provides the best solution for the destriped image. Image (c) is over regularized whereas image (d) is not sufficiently regularized. Image (f) represents the percentage error between images (a) and (e).

References

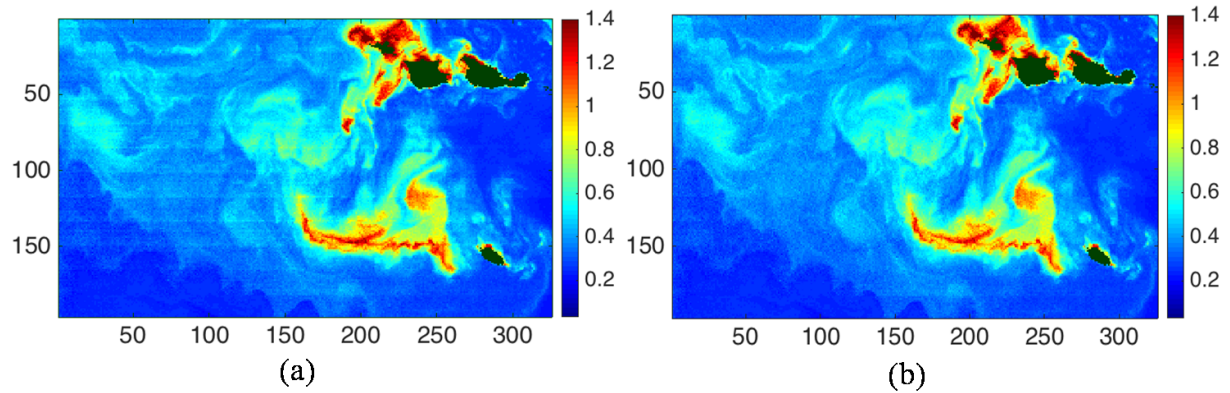


Figure 8. Image (a) shows the destriped image scene of the image (a) in Fig. ?? from NASA's vicarious calibration of L2 (*.nc) products method. While the NASA's vicarious calibration of L2 (*.nc) products method does improve over the raw image, there are still stripe artifacts present. The following image (b) represents the destriped image of the image (a) from our method.

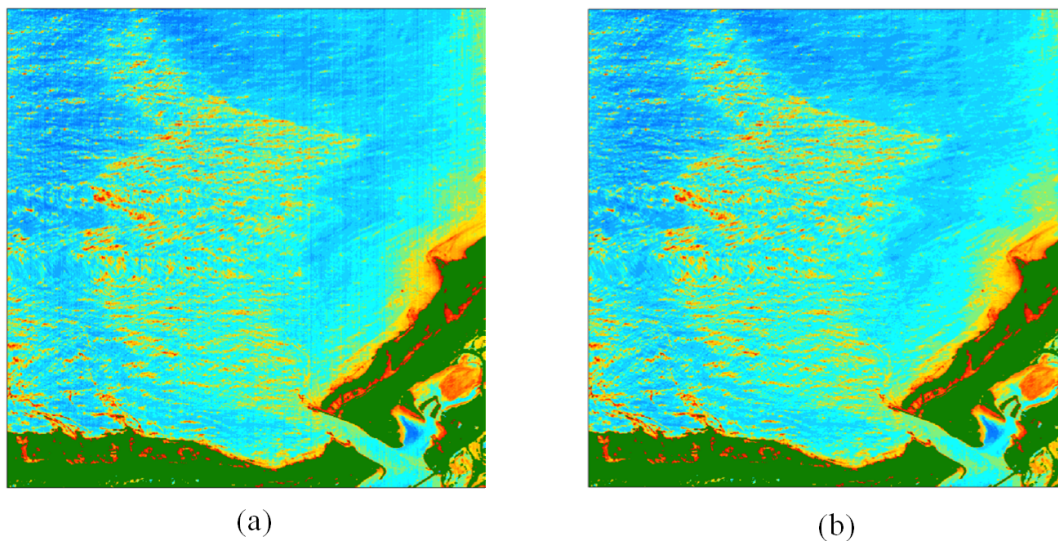


Figure 9. Image (a) is band 22 ($\lambda 410$ nm) of a hyperpectral image which was taken from JPL PRISM ?. The stripe pattern is vertical and the destriped images shown in image (b). Green represents the land of the observed region.